Sādhanā Vol. 28, Parts 1 & 2, February/April 2003, pp. 23–45. © Printed in India

Structure and thermal stability of nanocrystalline materials

B S MURTY, M K DATTA and S K PABI

Department of Metallurgical and Materials Engineering, Indian Institute of Technology, Kharagpur 721 302, India
e-mail: bsm@iitkgp.ernet.in

Abstract. Nanocrystalline materials, which are expected to play a key role in the next generation of human civilization, are assembled with nanometre-sized "building blocks" consisting of the crystalline and large volume fractions of intercrystalline components. In order to predict the unique properties of nanocrystalline materials, which are a combination of the properties of the crystalline and intercrystalline regions, it is essential to understand precisely how the structures of crystalline and intercrystalline regions vary with decrease in crystallite size. In addition, study of the thermal stability of nanocrystalline materials against significant grain growth is both scientific and technological interest. A sharp increase in grain size (to micron levels) during consolidation of nanocrystalline powders to obtain fully dense materials may consequently result in the loss of some unique properties of nanocrystalline materials. Therefore, extensive interest has been generated in exploring the size effects on the structure of crystalline and intercrystalline region of nanocrystalline materials, and the thermal stability of nanocrystalline materials against significant grain growth. The present article is aimed at understanding the structure and stability of nanocrystalline materials.

Keywords. Nanocrystalline materials; nanocrystalline structure; thermal stability; metastable phases.

1. Introduction

Interest in materials that are an assemblage of nanometre-sized "building blocks", arises from the realization that by controlling the sizes of such "building blocks" (in the range of 1–100 nm, the level of atoms, molecules and supramolecular structures) one begins to alter a variety of the physical, mechanical, and chemical properties of bulk materials (Pabi & Das 1997; Siegel *et al* 1999; Roco *et al* 2000). For example, even a cooperative phenomenon such as melting point and melting thermodynamic functions (enthalpy and entropy of melting) could be affected in nanometre-sized "building blocks" materials compared to coarse-grained polycrystalline materials (Lai *et al* 1996; Schmidt *et al* 1998). The evidence of systematic decrease of the average melting temperature (T_m) and normalized heat of fusion (ΔH_m) with decrease of particle size is shown in figure 1 for nanometre-sized Sn particles. These assembled materials, of single or multi-phase systems, with "building blocks" in the nanometre range are called *nanocrystalline*, *nanostructured* or *nanophase* materials. Several categories of

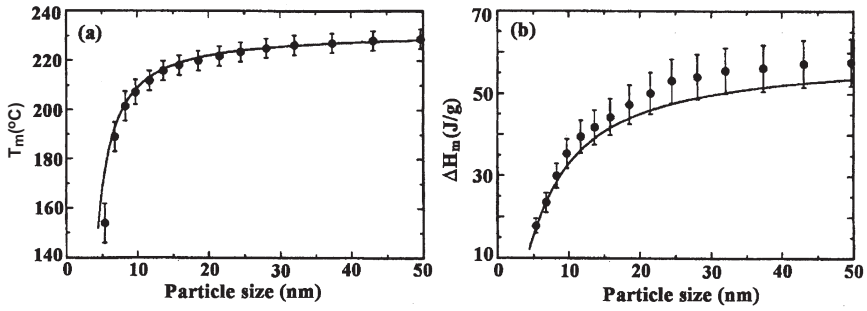

Figure 1. Size dependence of the **(a)** melting point (T_m), and **(b)** normalized heat of fusion (ΔH_m) of Sn nano-particles (Lai *et al* 1996).

nanocrystalline materials, like zero-dimensional atom clusters and cluster assemblies, one and two-dimensionally modulated multilayers and overlayers, and three-dimensional equiaxed nanocrystalline structures, can be produced by various techniques (Hadjipanayis & Siegel 1994; Gleiter 1995; Lu 1996; Murty & Ranganathan 1998; Suryanarayana 2001) as shown in table 1. Synthesis, characterization and processing of different categories of nanocrystalline materials are part of an emerging and rapidly growing field referred to as *nanotechnology*. Advances in nanoscience and nanotechnology are expected to have major impact on human health, wealth and security in the coming decades (Roco *et al* 2000; Roco & Bainbridge 2001). Among the expected breakthroughs are orders of magnitude increases in computer efficiency, human organ restorations using engineered tissues, "designer" materials created from directed assembling of atoms and molecules, and emergence of entirely new phenomena in chemistry and physics.

The basic idea of nanocrystalline materials in which 50% or more of the atoms are situated in the grain boundaries, was proposed by Gleiter's group in 1981 (Gleiter 1981). Figure 2 shows a schematic illustration of a hard sphere two-dimensional model of a hypothetical nanocrystalline material (Gleiter 1995; Gleiter 2000). There are two types of atoms in the nanocrystalline structure: crystal atoms with neighbour configuration corresponding to lattice and boundary atoms with a variety of interatomic spacings. Thus, materials assembled with nanometre-sized "building blocks" are *microstructurally heterogeneous* consisting of the crystallites and regions between adjacent crystallites, i.e. intercrystalline components. According to phase mixture model (Wang *et al* 1995; Kim *et al* 2000), any property of nanocrystalline materials can be presented by simple rule of mixtures, i.e. $X = V_{cr}X_{cr} + V_{ic}X_{ic}$ where subscripts cr and ic refer to the crystalline and intercrystalline components of nanocrystalline

Table 1. Classification and synthesis techniques of nanocrystalline materials (Gleiter 1995).

Dimensionality	Synthesis techniques
Zero	Sol-gel, chemical route
One	Vapour deposition, electro deposition
Two	Chemical vapour deposition
Three	Gas condensation, severe plastic deformation

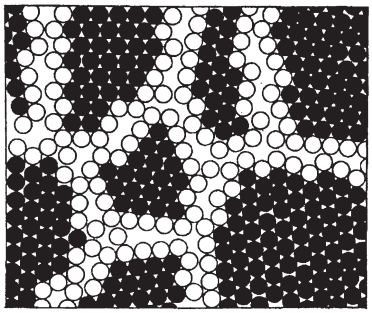

Figure 2. Two-dimensional model of nanocrystalline material. Atoms in the crystalline region are indicated as black circles, while those in the interface regions are represented as open circles (Gleiter 1996, 2000).

materials, and X and V denote the property and volume fraction of respective components. Intercrystalline components include interface/grain boundaries, triple lines and quadruple nodes. Taking a cubic unit cell or a regular polyhedron unit cell of nanocrystalline material, the volume fraction of each component can be expressed as follows (Kim *et al* 2000):

$$V_{cr} = (d - \delta^3)/d^3,\ V_{gb} = 6(d - \delta)^2(\delta/2)/d^3,\ V_{tj} = 12(d - \delta)(\delta/2)^2/d^3,\ V_{qn} = \delta^3/d^3,$$

where subscripts cr, gb, tj and qn refer to crystallite, grain boundary, triple lines and quadruple nodes respectively, and d and δ represent the crystallite size and the grain boundary thickness. Figure 3 represents the variation of volume fraction of intercrystalline components with crystallite size of grain boundary thickness $\sim$ 1 nm (which is the generally accepted value). From figure 3, it is evident that when crystallite size is smaller than about 20 nm, the total volume fraction of the intercrystalline region (grain boundary, triple junctions and quadruple node) becomes significant. It should also be noted that the volume fraction of the crystallite decreases rapidly below about $\sim$ 20 nm. Therefore, in order to predict the performance of a particular device or component based on nanocrystalline materials, it is essential to understand precisely how the structure of the intercrystalline region, as well as the structure of the crystallites varies with decrease in crystallite size. Ultimately, these studies would also define the practical lower limit down to which miniaturization in such devices is possible.

In addition, study of thermal stabilities of nanocrystalline materials against significant grain growth is of both scientific and technological interest because in most of the synthesis techniques, the nanocrystalline materials are produced in powder form, which have to be consolidated to obtain dense material for potential use. Choice of pressures and temperatures for consolidation will depend on the thermal stability of the nanocrystalline materials against

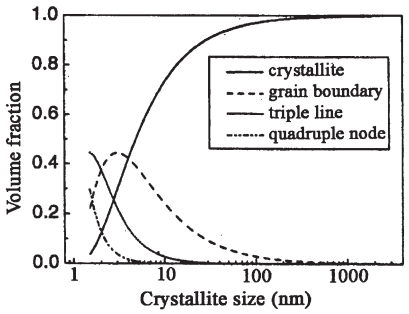

Figure 3. Volume fraction of the crystallite, grain boundary, triple line and quadruple node as a function of grain size (Kim *et al* 2000).

significant grain growth. A compromise between good interparticle or intercrystalline bonding and minimum porosity on the one hand, and a minimized coarsening of the grain structure on the other has to be made. In almost all studies (Hague & Mayo 1997; Kanters *et al* 2000), it has been reported that fully dense material (densities close to the theoretical values) in nanocrystalline materials cannot be obtained without a sharp increase in grain size (to micron level), which may consequently result in the loss of some of the unique properties of nanocrystalline materials. Therefore, extensive interest has been generated in exploring the size effects on the structures of the crystalline and intercrystalline regions of nanocrystalline materials, and on the thermal stabilities of nanocrystalline materials against significant grain growth. The present article reviews the present states of understanding in these aspects of nanocrystalline materials.

2. Structure of intercrystalline region

Among the intercrystalline components (interface/grain boundary, triple junctions and quadruple node), the interface/grain boundary between neighbouring crystallites is assumed to be very important and a significant component of nanocrystalline materials in controlling the macroscopic properties of the sample (Hadjipanayis & Siegel 1994; Gleiter 1995; Lu 1996; Gleiter 2000). It has been reported in different systems that if the crystallites of two nanocrystalline materials of same element/compound have comparable size, chemical composition etc., the properties of both nanocrystalline materials may deviate significantly if their interfacial structure differs. For example, nanocrystalline Ni (crystal size of about 10 nm, density of about 94%) prepared by consolidation of Ni powder, obtained by inert gas condensation technique, exhibited little ($< 3\%$) ductility whereas nanocrystalline Ni (similar grain size and chemical composition) obtained by means electro-deposition could be deformed extensively ($> 100\%$) (Gleiter 2000). Therefore, extensive studies have been carried out for exploring the nature of interfaces in nanocrystalline solids, whereas only a few studies have been devoted to the triple junction and quadruple nodes. For this reason, the present article is concerned only with the structures of the interfaces in nanocrystalline materials.

Extensive investigations have been conducted on the structural characteristics of interfaces in nanocrystalline materials, made by different synthesis techniques, using X-ray diffraction (XRD), high resolution transmission electron microscopy (HREM), Mössbauer spectroscopy, positron annihilation spectroscopy (PAS), Raman scattering, extended X-ray absorption fine structure (EXAFS) and molecular dynamics computer simulations (Hadjipanayis & Siegel 1994; Gleiter 1995; Lu 1996; Gleiter 2000; Swygenhoven *et al* 2000). In spite of these studies, the structure of such interfaces has not yet been completely understood (Hadjipanayis & Siegel 1994; Gleiter 1995; Stern *et al* 1995; Lu 1996; del Bianco *et al* 1997; Balogh *et al* 2000; Gleiter 2000; Swygenhoven *et al* 2000). One exciting claim has been made that the interfacial region is completely disordered, as frozen gas, possessing neither the short-range order of liquids and amorphous solids nor the long-range order of crystals, and having a large excess volume of about 10–40% (Zhu *et al* 1987; Haubold *et al* 1989). The experimental basis for this claim was found in diffraction analysis, EXAFS analysis and Mössbauer spectroscopy investigations of nanostructured Fe, Cu, Co and Pd etc. (Zhu *et al* 1987; Haubold *et al* 1989; Loffler *et al* 1994). A wide range of interatomic spacings, consistent with a low degree of atomic short-range order, of the grain-boundary component of nanocrystalline Fe was deduced from a Mössbauer spectroscopy investigation (Zhu *et al* 1987; del Bianco *et al* 1997). The nearest-neighbour coordination number, calculated by measuring the pair correlation functions, in

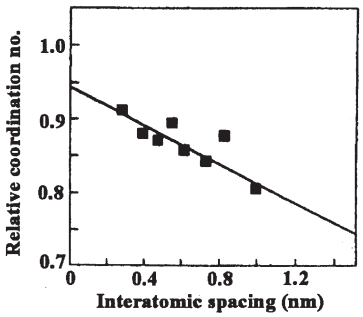

Figure 4. Coordination number for nanocrystalline Pd relative to a Pd single crystal as a function of the interatomic spacings (Loffler *et al* 1994).

the boundary regions of nanostructured Pd relative to Pd single crystal as a function of the interatomic spacings is shown in figure 4 (Loffler *et al* 1994). This result indicates large reduction in the atomic coordination number and atomic density at the boundary, supporting the idea of a very disordered structure at the interface. By molecular dynamic simulations of nanocrystalline materials, which can provide an atomistic view of the microstructures through the mean field approximation of atomic interactions, Phillpot, Wolf and their coworkers (Phillpot *et al* 1995) and several others (Keblinski *et al* 1999; Gleiter 2000) have claimed low-density regions in the grain boundary, absence of long-range periodicity, narrower grain-boundary energy distribution, and larger grain-boundary width, with a narrow distribution as compared to bicrystals. Based on their simulations, they have suggested a simple structural model for grain boundaries in nanocrystalline materials based on a "cement-like" phase, reminiscent of Rosenhain's amorphous-cement model. In these studies, the nanocrystalline interface structure is claimed to be different from that in conventional polycrystals.

On the other hand, a number of other investigations based on HREM, EXAFS and Mössbauer spectroscopy of the interface in several nanocrystalline samples indicate that the grain boundaries are well-ordered structures of low energy configuration, similar to those determined for coarse-grained polycrystalline or bicrystalline materials (Stern *et al* 1995; Lu 1996; Zhao *et al* 1999; Swygenhoven *et al* 2000; Balogh *et al* 2000). EXAFS measurements on nanocrystalline Se samples with crystallite size ranging from 13 to 60 nm Zhao *et al* (1999) concluded that, with refinement of crystallite size, the intrachain structure (the bond length, the coordination number) is unchanged while the interchain spacing is enlarged. This result suggests that the grain boundary in the nanocrystalline Se is in a low-energy configuration that is different from the disordered "gas-like" grain boundary structure. Stern *et al* (1995) studied nanocrystalline Cu (13 nm) by the total electron yield technique and found that the grain boundary structure, on the average, are similar to that in conventional polycrystalline Cu, contrary to previous EXAFS measurements which indicated a lower coordination number (Haubold *et al* 1989). In the polymorphous and eutectic nanocrystallization products of $Ni_{33}Zr_{67}$ and Ni–P respectively, flat interfaces of low energy configurations with very small excess volume were observed in the HREM images (Lu 1996). Careful analysis of spectral contribution of Mössbauer spectra of the possible impurities and chemical mixing at interfaces, Balogh *et al* (2000) have reported that the grain boundary of nanocrystalline Fe is similar in nature to polycrystalline Fe whereas no grain boundary phase with very distorted structure or highly reduced density has been detected. For nanocrystalline Ni–P materials with average grain sizes ranging from a few nanometres to 60 nm, it was found that the average interfacial excess energy (ΔE_{in}) and interfacial excess volume (ΔV_{in}) decreases significantly with a reduction of grain size in an approximately linear fashion, as shown in figure 5 (Lu *et al* 1993;

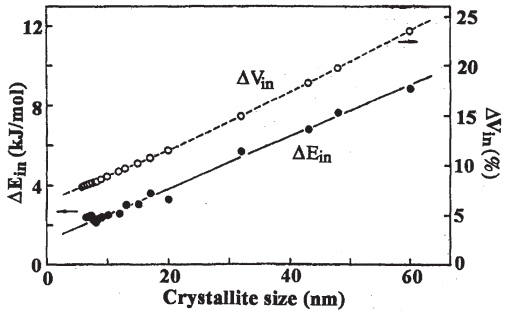

Figure 5. Variation of the interfacial excess energy (ΔE_{in}) and excess volume (ΔV_{in}) with the average grain size in the nanocrystalline Ni–P alloy (Lu *et al* 1993; Lu 1996).

Lu 1996). A similar decreasing tendency of grain boundary energy with reduction of crystallite size was detected in TiO_2 nanocrystalline materials made by use of the ultrafine particle (UFP) consolidation method (Terwillingner & Chiang 1993), and in nanocrystalline Se produced by controlled crystallization of amorphous Se (Lu & Sun 1997). Swygenhoven *et al* (2000) have presented a detailed analysis of both low angle and high angle grain boundary structures in computer-generated Cu and Ni three-dimensional nanocrystalline samples with crystallite sizes in the range of 5–12 nm. A significant degree of crystalline order is found for all the boundaries studied. The above evidences indicate that the interfaces in nanocrystalline materials appear to have essentially the same structure as those found in coarse-grained materials. No disordered interfaces with high energetic configurations were detected in these studies.

Excellent work in nanostructured Pd by Loffler & Weissmüller (1995) and in nanostructured Ni_3Fe by Frase *et al* (2000), in different consolidation, aging and annealing conditions indicates that the atomic structures of relaxed grain boundaries are rather similar to those determined for coarse grained polycrystalline or bicrystalline materials, whereas the non-equilibrium (unrelaxed) grain boundaries differ significantly from those in coarse grained materials. In the case of the sintering of two isolated Cu nanoparticles, a case of minimum imposed constraints in molecular simulation; Zhu & Averback (1996) have reported that the large surface-to-volume ratio generates strong enough driving forces to induce rotation, plastic deformation, and densification. As a consequence, they have concluded that a low angle grain boundary results even for random initial misorientation. Introducing more constraints in simulation, simultaneous sintering of several Pt particles at different applied pressure was analysed by Liu *et al* (1994). They have reported several phenomena such as surface rounding, neck formation, void formation and shrinkage and cluster extrusion. The resulting grain boundaries are very narrow and exhibit only localized disorder. This could occur because of a combination of local deformation and diffusional processes that allow low energy configurations to result. These results suggest that the atoms in nanocrystalline materials are sufficiently mobile to rearrange themselves into low energy configurations that depend on the grain size. It is quite firmly established that the structure and properties of the grain boundaries depend on how the materials were prepared (equilibrium or nonequilibrium techniques) and how the materials are subsequently thermally treated.

3. Structure of nanometre-sized crystallites

The lattice structure of nanometre-sized crystallites in nanocrystalline samples synthesized by various methods was studied by means of the quantitative XRD and Mössbauer spectroscopy. The results showed that the lattice structure of the nanometre-sized crystallites evi-

Table 2. A list of the lattice parameter changes ($\Delta a = (a - a_0)/a_0$ and $\Delta c = (c - c_0)/c_0$) and the static DWP changes ($\Delta B_s = (B_s - B_{s0})/B_{s0}$) in various nanocrystalline samples processed by different techniques (Lu & Zhao 1999).

			Lattice distortion		
Sample	d (nm)	Synthesis route*	Δa	Δc(%)	ΔB_s(%)
Cr	11	UFP	0·04	-	230
Fe	8	BM	0·09	-	110
Cu	11	BM	0·06	-	-
Cu	27	ED	0·06	-	-
Pd	8	UFP	0·04	-	220
Si	8	BM	0·20	-	-
Ge	4	BM	0·20	-	-
Se	13	CL	0·30	−0·12	900
Se	14	BM	0·15	−0·01	-
Ni_3P	7	CL	0·21	−0·13	-
Fe_2B	23	CL	0·20	−0·23	-

UFP = ultrafine powder consolidation; BM = ball milled;
ED = electrodeposition; CL = crystallization from amorphous solids

dently deviates from the equilibrium state. The deviation may be classified as: (i) distorted lattice structures in pure elements and stoichiometric line compounds, and (ii) formation of metastable phase below a critical crystallite size.

3.1 *Distorted lattice structure*

Lattice distortion in various nanocrystalline materials, processed by means of different approaches, is manifested by a significant change in the lattice parameter (Lu 1996; Lu & Zhao 1999), Debye–Waller parameter (DWP) (Zhao & Lu 1997; Lu & Zhao 1999) and characteristic Debye temperature (Zhao & Lu 1997; Herr *et al* 1998; Lu & Zhao 1999). Table 2 summarizes the experimental data of lattice distortion (lattice parameter and DWP) in nanocrystalline materials reported in the literature.

Quantitative XRD measurements of the unit cell volume, for nanometre-sized Ni_3P (*bct*) and Fe_2B (*bct*) (Lu 1996), showed that it is enlarged (as much as 0·3%) with refinement of grain size with respect to the corresponding equilibrium value (see figure 6), i.e., the lat-

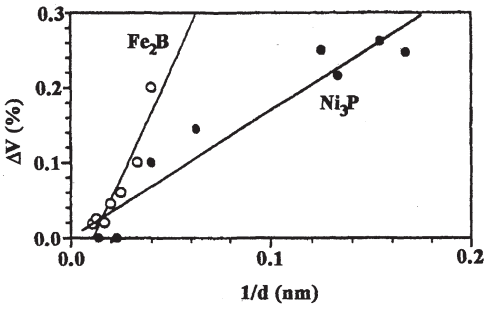

Figure 6. The variation of relative unit cell volume ($\Delta V = V/V_0 - 1$) with reciprocal crystallite size ($1/d$) for Ni_3P and Fe_2B (Lu 1996).

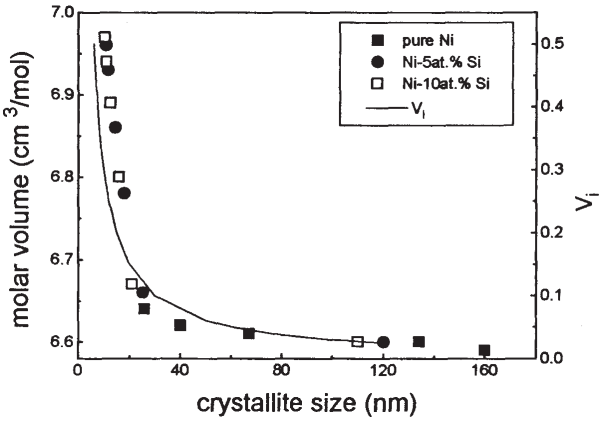

Figure 7. Variation of molar volume and grain boundary volume fraction (V_i) with refinement of crystallite size for Ni–Si blends ($0 \leq$ at. % Si ≤ 10) (Datta *et al* 2000a; Datta 2001).

tice of the nanometre-sized crystallite is dilated relative to the perfect crystal structure. In nanocrystalline elemental Si and Ge with mean grain size of about 8 nm, made by high-energy ball milling, the lattice parameter was found to increase by 0·2% with respect to the single crystal (Gaffet *et al* 1991). In nanocrystalline pure selenium crystallized from melt-quenched amorphous Se and/or synthesized by high-energy ball milling, evidence of lattice distortion was also detected (Zhao & Lu 1997). The expansion of lattice parameter also has been detected in nanocrystalline *bcc* (Cr, Fe, Nb) (Lu & Zhao 1999; Chatterjee *et al* 1999) and *fcc* (Ni, Cu, Ag, Pd) (Gamarnik 1991; Liu *et al* 1994; Lu & Zhao 1999; Datta *et al* 2000) metals synthesized by means of different approaches. A significant lattice expansion of nanocrystalline *fcc* Ni(Si) is evident during mechanical alloying when the crystallite size is refined below $\sim$ 20 nm, as shown in figure 7 (Datta *et al* 2000a). A molar volume expansion (6·59 to 6·97 cm^3/mol) of 0·38 cm^3/mol (5·8%) is evident for *fcc* Ni(Si) when the crystallite size decreased from the bulk state to $\sim$ 10 nm. Expansion of molar volume of *fcc* Ni(Si), compared to that of single crystal, with refinement of crystallite size has been explained by considering the presence of a stress field at the core due to presence of vacancy or vacancy cluster situated at the grain boundary in nanocrystalline material, which mainly depends on the volume fraction of the interface ($V_i = 3\delta/d$) that is inversely related to crystallite size ($1/d$) (Datta 2001). The volume fraction of the grain boundary, $V_i(3\delta/d)$, is plotted in figure 8 by taking into account the grain boundary thickness (δ) as 1 nm in the whole range of crystallite size. A significant increase in V_i, i.e. the stress field, is predicted below $\sim$ 20 nm of crystallite size, which is in good agreement with experimental result. Increase of lattice parameter with an approximate $1/d$ rule has also been reported in ball-milled nanocrystalline Cu, Fe, Ni_3P and Fe_2B (Lu 1996; Lu & Zhao 1999). In most transition metal oxides, a decrease in the crystallite size is accompanied by an increase in the lattice parameter, leading to an enhancement in the unit cell volume. Unit cell volume of 8 nm γ-Fe_2O_3 nanoparticles was found to be 2·6% higher than the bulk cell volume (Ayyub *et al* 1988). The static DWP in various nanocrystalline samples, which reflects the static atomic displacement, increases by $\sim$ 100–900% compared to the equilibrium values, as listed in table 2. It was found that the static DWP normally increases significantly with a reduction of grain size with a $1/d$ rule, while the temperature-dependent thermal DWP shows no measurable grain size dependence in nanocrystalline materials (Eastman & Fitzsimmons 1995; Zhao & Lu 1997). This behavior verifies the existence of the lattice distortion in the nanocrystalline lattice. Also, a number of researchers (Hong *et al* 1995; Zhao & Lu 1997; Herr *et al* 1998; Lu & Zhao

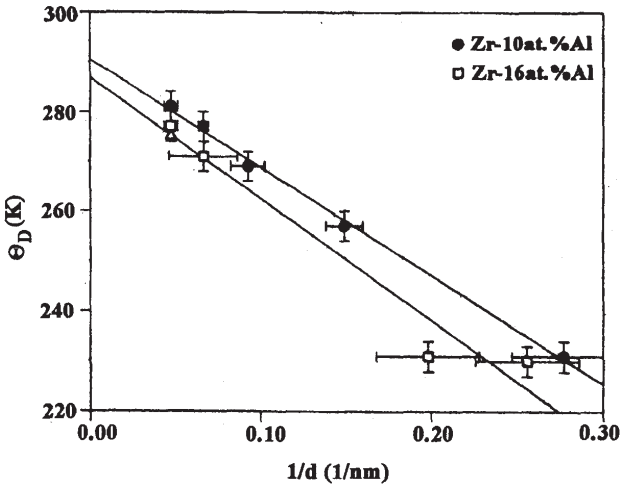

Figure 8. Debye temperature (Ω_D) against reciprocal grain size ($1/d$) of the Zr–10 at. % Al and Zr–16 at. % Al samples (Herr *et al* 1998).

1999) have identified that the characteristic Debye temperature (Ω_D), calculated from low temperature specific heat measurement, decreases significantly for nanocrystalline materials with a reduction in crystallite size, as shown in figure 8 for nanocrystalline $Zr_{1-x}Al_x$ solid solution. The depressed Debye temperature in nanocrystalline samples implies a decrease in the cohesion of atoms in the nanocrystallites, which agrees well with the measured grain size dependence of static DWP and lattice parameters (unit cell volume expansion). The intrinsic reason for the lattice distortion and expansion in pure element nanocrystallites and stiochiometric line compound nanophases, which have no solubility of other elements in the equilibrium state, is still not known. A few researchers have used the concept of expansive stresses due to the presence of inter-dipolar repulsion at the surface (Ayyub *et al* 1988; Gamarnik 1991) or the presence of stress field caused by the vacancies and vacancy cluster situated at the grain boundaries (Lu 1996; Qin *et al* 1999; Datta *et al* 2000).

3.2 *Formation of metastable phases*

Another effect related to the reduced size of the crystallites in nanocrystalline materials concerns the formation of metastable phase in nanocrystalline state. Similar to thin films and needle-like crystals, the thermodynamic conditions of phase equilibrium in nanocrystals alter due to significant contribution of the interfacial energy to the energetic balance and new phases unusual in a bulk state may appear (Grayznov & Trusov 1993; Zu 1996; Murty & Ranganathan 1998; Gleiter 2000). For example, Datta *et al* (2000b) have recently reported that only congruent melting phases, $Ni_{31}Si_{12}$, Ni_2 Si and NiSi form, while the formation of non-congruent melting phases, Ni_3Si, Ni_3Si_2 and $NiSi_2$, does not take place during mechanical alloying in the Ni–Si system in the course of generating nanocrystalline materials ($\sim$ 10–15 nm), even at the corresponding equilibrium phase fields, as shown in figure 9 of metastable phase fields of Ni–Si system. As a result, different cooperative phenomena such as magnetism, ferroelectricity and superconductivity should be affected considerably by size reduction. Therefore, it is very important to study the metastable phase formation with reduction of crystallite sizes.

3.2a *Allotropic transformations:* Structural transformation to other crystal structures has been identified in a number of pure metals and compounds, synthesized by different tech-

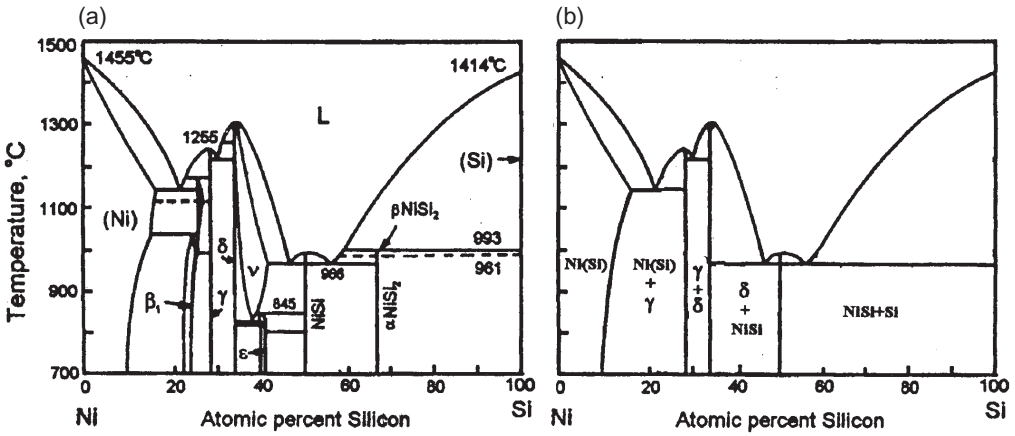

Figure 9. **(a)** Equilibrium and **(b)** metastable phase diagram of Ni–Si system showing the phase fields in bulk and nanocrystalline state respectively, after MA (Datta *et al* 2000b).

niques, below a critical crystallite size. Experiments have shown that nanoparticles of pure metals, Nb, Mo, W, Fe, and Ta, with crystallite sizes 5–10 nm have close packed *hcp* or *fcc* lattices instead of their stable *bcc* structure observed in the bulk state (Grayznov & Trusov 1993; Chatterjee *et al* 1999). An allotropic transformation from stable *fcc* Ni(Si) to metastable *hcp* Ni(Si) has been identified during mechanical alloying below a critical crystallite size of $\sim$ 10 nm, as shown in the XRD patterns in figure 10 (Datta *et al* 2000a). A transition from *bcc* Nb(Al) to *fcc* Nb(Al) has been reported by Chattarjee and others (Chatterjee *et al* 1999; Chattopadhay *et al* 2001) in the nanocrystalline state. Manifestations of these effects have also been detected in intermetallics and oxide-based systems. The high temperature metallic phase α-$FeSi_2$ becomes stable below a critical crystallite size instead of equilibrium low temperature semiconducting material β-$FeSi_2$ (Gaffet *et al* 1993). In the iso-structural system of Fe_2O_3 and Al_2O_3, the rhombohedral (α) phase becomes unstable when the crystallite size is made sufficiently small ($<$ 30 nm) and the metastable cubic (γ) phase of more open structure with a substantially larger unit cell volume is preferentially nucleated (Ayyub *et al* 1988; Grayznov & Trusov 1993; Liao *et al* 1998). It has also been reported that the smaller particles of TiO_2, known to occur in three crystallographic modifications: rutile, brookite and

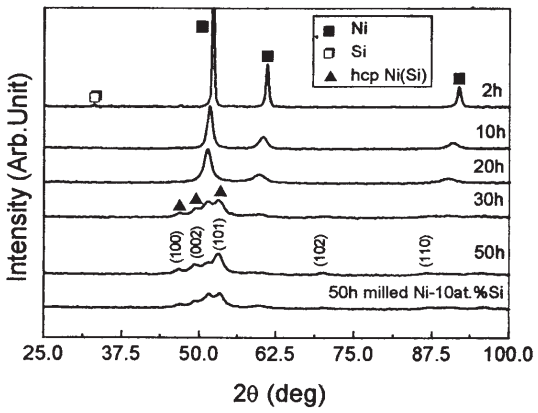

Figure 10. XRD patterns of Ni–Si blends (5 and 10 at %Si) showing transformation of *fcc* to *hcp* Ni(Si) during MA (Datta *et al* 2000a).

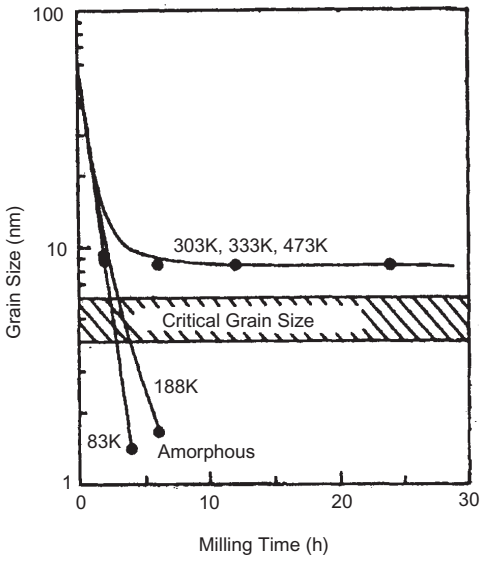

Figure 11. Grain size vs milling time for CoZr milled at different temperatures in a Spex mill. The shaded area represents the grain size below which the alloy becomes amorphous (Koch 1996; Suryanarayana 2001).

anatase, tend to be nucleated preferentially as anatase, whereas larger particles are produced in the form of rutile (Ding & Liu 1997; Liao *et al* 1999). Similarly, in the case of ZrO_2 (bulk state has monoclinic symmetry), it has been observed that the normally unquenchable high-temperature tetragonal phase becomes stable at room temperature when the particle size is less than 10 nm and, above this critical size, tetragonal to monoclinic transformation occurs (Garvie 1965; Chraska *et al* 2000). $PbTiO_3$ and $BaTiO_3$, which are ferroelectric in bulk state with tetragonal structure, do not exhibit any ferroelectric transition on heating below a critical crystallite size of about 20 nm, suggesting that the crystal becomes cubic below this critical crystallite size (Ayyub *et al* 1995; Beck *et al* 1999). A similar situation is also observed in the high T_c superconducting oxides. There is a tendency for the structure of the orthorhombic superconducting phase $YBa_2Cu_3O_{7-\delta}$ to become tetragonal with decreasing crystallite size, and this leads to a progressive decrease in the T_c and finally to the loss of superconductivity at small enough sizes (Ayyub *et al* 1995).

3.2b *Amorphization:* Evidence of amorphization below a critical crystallite size in nanocrystalline materials has been reported on large number of alloy systems (Koch 1996; Murty & Ranganathan 1998; Gleiter 2000; Suryanarayana 2001). For example, amorphization of intermetallic compound CoZr has been identified below a critical crystallite size during high-energy ball milling at cryogenic temperature (see figure11) (Yamada & Koch 1993; Koch 1996). The band shown in figure 11 represents the critical crystallite size, below which amorphization occurs. Similar results were reported for NiTi and $NiZr_2$ intermetallics (Yamada & Koch 1993; Koch 1996). While most studies of amorphization of single composition materials have focused on intermetallic compound or, in some cases, non-metallic inorganic compounds, there are also a few reports on amorphization of pure elements. Crystal to amorphous transformation has been observed for some metalloid (C, Se and graphite) and covalent semiconducting elements, Si and Ge, below a critical crystallite size of few nanometres synthesized by a variety of methods including ion implantation, vapour deposition or high-energy ball-milling technique (Veeprek *et al* 1982; Gaffet & Hermalin

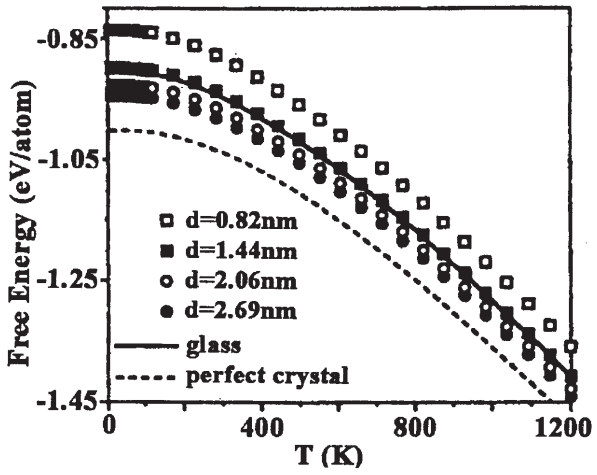

Figure 12. Comparison of temperature dependence of the total free energy of nanocrystalline Cu with a Lennard–Jones glass and perfect crystal (Wolf *et al* 1995; Gleiter 2000).

1990; Fukunaga 1995; Guo & Lu 1998). In contrast to metalloid and covalent elements, metallic elements in general do not exhibit amorphization, except for certain transition elements (Ni, Co, Cr, Fe, Mn) that subsequently have to be kept below 20K to maintain the amorphous state (Chanderis *et al* 1990). Because elementally pure amorphous materials are disordered locally, but not chemically, they can very easily crystallize well below ambient temperature and it has generally been accepted that amorphous pure metals do not exist, at least at temperatures near room temperature. Free energy and lattice-dynamics simulations of nanocrystalline pure elements and related glasses suggest that nanocrystalline elements are unstable relative to glass below a critical crystallite size of around $\sim$ 2 nm (Wolf *et al* 1995; Gleiter 2000). Figure 12 shows the temperature dependence of the free energy of nanocrystalline Cu of different grain sizes, which shows that nanocrystalline Cu is unstable relative to glass below a critical crystallite size of about 1·4 nm. Formation of this low level of crystallite size is very difficult for pure metallic elements. However, in presence of solute elements, crystallite size could be refined to lower levels than pure metallic elements, and it has been found that the ultimate grain size of solid solution decreases with increasing solute concentration and it could be possible to reach as low as $\sim$ 2 nm (Weissmuller *et al* 1992; Koch 1997). Therefore, the amorphous phase of nanocrystalline metallic elements could be stabilized in presence of solute elements, which has also been triggered due to alloying effect superposition with nanocrystalline effects (Koch 1996; Herr *et al* 1998). Datta *et al* (2002) has suggested that a critical crystallite size of $\leq$ 10 nm and a critical lattice strain of $\geq$ 1·28% are the prerequisites for the amorphization of *bcc* Fe(Si) solid solution, up to 25 at.% Si (see figures 13a and b). In the case of pure Fe, the critical values of crystallite size and lattice strain could not be achieved within 30h of mechanical alloying, and it has been identified that the crystallite size of pure Fe becomes saturated at around $\sim$ 20 nm after long milling time. The extrapolation of the experimental to zero (see figure13) apparently indicates that even pure Fe may undergo amorphization if its crystallite size and lattice strain are brought to the level of $<$ 10 nm and $>$ 1·28% respectively. The formation of amorphous phase in pure Fe (at least in the grain boundary), as reported by Bianco *et al* (1998) for the average crystallite size of $\sim$ 10 nm during the high-energy ball milling technique strengthens the above proposition.

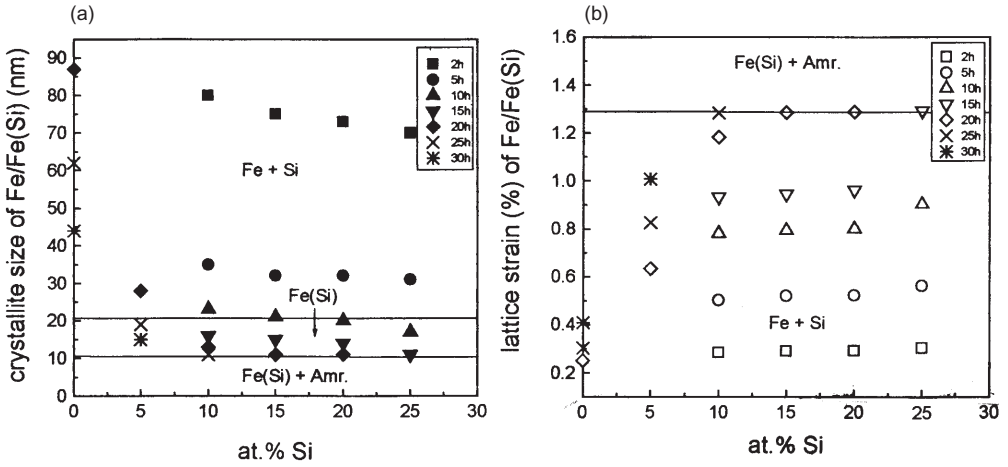

Figure 13. Variation of **(a)** crystallite size (nm), and **(b)** lattice strain (%) of Fe-Si system with composition at different milling times (Datta *et al* 2002).

3.3 *Supersaturated solid solutions*

Due to the Gibbs–Thomson effect, solubilities of solutes are expected to be much enhanced in solid solution, with grain refinement down to the nanometre regime. Enhanced solubilities have been experimentally observed in nanocrystalline materials produced by different synthesis techniques. For instance, Mutschele & Kirchheim (1987) found that the solubility of H in nanocrystalline Pd sample (at a concentration of 10^{-3} or below) is increased by a factor of 10 to 100 relative to a Pd single crystal. Similar effect was reported by Hahn *et al* (1990) for the solubility of Bi in nanocrystalline Cu, which reaches about 4% at 373 K, while the equilibrium solubility of Bi in Cu single crystal is negligible (less than 10^{-4}). Even if the constituents are immiscible in the solid and/or molten state (e.g., Fe–Ag), the formation of solid solution in the nanocrystalline state has been noticed (Herr *et al* 1990). Other experimental evidences, such as the formation of Cu–Fe, W–Ga and Cu–W (Yavari *et al* 1992; Klassen *et al* 1997; Gleiter 2000) solid solutions in the nanocrystalline state, imply that an intrinsic enhancement of solid solubility is possible in nanocrystalline samples. In the nanocrystalline state, solute atoms are known to segregate to the boundaries forming a solute cloud in the vicinity of the boundary. Therefore, the solid solubility in the grain boundaries differs considerably from that in the interior of the crystals. As a consequence of solute enrichment at the grain boundaries and of the large specific grain boundary area, theory and experiments (Weissmuller *et al* 1992; Gleiter 2000) show that nanocrystalline materials have an enhanced overall solubility for solutes with large heat of segregation. Hodaj & Desra (1996) have explained the stability of metastable solid solutions against homogeneous and heterogeneous nucleation of the stable intermetallic phase based on thermodynamic arguments of the concentration gradient field. According to Desra's model (Yavari *et al* 1992; Hodaj & Desra 1996), below a critical concentration there is no driving force for nucleation of metastable solid solutions to stable intermetallics, if the tangents below a critical concentration do not intersect the free energy curve of the intermetallic, which leads to the definition of a critical concentration gradient beyond which nucleation of intermetallic is not allowed and an extension of solid solubility up to this critical concentration is expected. Pabi *et al* (2001) have observed wide phase fields for the Ni aluminides

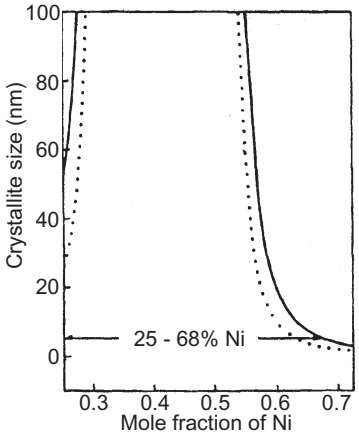

Figure 14. Variation of NiAl phase field with crystallite size.

in the nanocrystalline state and could correlate the large extension in the NiAl phase field to its crystallite size based on thermodynamic calculations (see figure 14). The figure also gives the phase field of NiAl with a crystallite size of about 5 nm obtained by mechanical alloying (25-68%Ni), which compares quite well with thermodynamic calculations.

4. Mechanism of metastable phase formation in nanocrystalline state

Several theoretical concepts have been developed to understand the structural transformation in the course of generating nanocrystalline materials synthesized by different processing techniques. Based on the analysis of the available literature, all of the theoretical work can be subdivided into atomistic and thermodynamic models (Johnson *et al* 1993; Ettl & Samwer 1994; Yavari 1994; Desra 1996; Koch 1996; Herr *et al* 1998; Gleiter 2000).

4.1 *Atomistic models*

Atomistic models are capable of describing crystal to amorphous or other crystal structure transformation, which can take place in a wide range of materials by means of various solid-state techniques. Despite the variety of techniques, there appears a common observation that lattice atoms are displaced from their equilibrium lattice sites, causing lattice strain and the softening of shear elastic constants (phonon instability) during the progress of transformation (Johnson *et al* 1993; Koike 1993; Ettl & Samwer 1994; Ikeda *et al* 1999). A number of experimental and theoretical results (Johnson *et al* 1993; Koike 1993; Ettl & Samwer 1994; Ikeda *et al* 1999) have shown that amorphization occurs when the crystal is strained to a material-dependent critical value, resulting in material-independent large decrease (40–50%) in the shear elastic constant. The prerequisites of this solid-state phase transformation, namely lattice strain and shear softening, can be obtained by the presence of static disordered in the parent crystal, which can be achieved either by forming supersaturated solid solution (Johnson & Fecht 1988) or by the accumulation of defects (Fecht 1992). As atomic displacement in the nanocrystalline materials is higher than in coarse-grained materials, it is expected that nanocrystalline materials have significant effect on shear softening to induce phase transformation below a critical crystallite size (Ettl & Samwer 1994; Koch 1996; Herr *et al* 1998). Recently, Datta *et al* (2000a) have explained the structural transformation of fcc

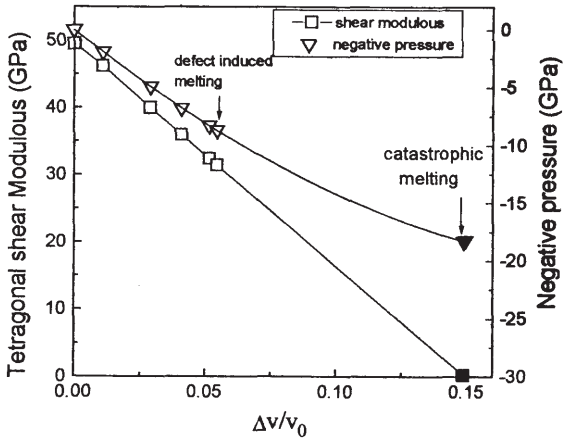

Figure 15. Variation of shear modulus and negative pressure of *fcc* Ni(Si) as a function of excess volume (Datta *et al* 2000a).

to *hcp* Ni(Si) below the critical crystallite size of around $\sim$ 10 nm by the mechanical instability concept. Calculations based on the equation of state show 37% reduction in tetragonal shear modulus of nanocrystalline *fcc* Ni(Si) at the onset of transformation (see figure 15) suggesting defect-induced melting of *fcc* Ni(Si) to amorphous structure of zero shear modulus, which is expected to be relaxed to *hcp* structure of molar volume 7·57 cm^3/mol, and is in good agreement with the molar volume of liquid at the melting point of Ni. They have also reported that a negative hydrostatic pressure of 8·7 GPa has been generated at the onset of transformation. Substitution of $P = 8{\cdot}7$ GPa and $\Delta V = 0{\cdot}60\,cm^3$/mol, yields an enthalpy change of 5·2 kJ/mol for *fcc* to *hcp* transformation, which is close agreement with the DSC result.

4.2 *Thermodynamic concepts*

A number of methods, from first principle calculations to empirical models, have been applied to understand the metastable phase formation in nanocrystalline materials (Yavari 1994; Desra 1996, 1997; Datta *et al* 2000a,b). The fundamental difference between coarse grain and nanocrystalline materials lies in the formation of large volume fraction of interfaces in nanocrystalline materials that has significant influence on the thermodynamics of phase formation/transformation. In the bulk state, the thermodynamic condition for phase α to be stable over metastable phase β is that $G_\alpha < G_\beta$. In case of nanocrystalline materials, the contribution of interfacial energy term (G_{int}) to the free energy cannot be neglected as in coarse-grained polycrystalline materials. The interfacial free energy of nanocrystalline materials, can be expressed as (Yavari 1994),

$$\Delta G_{\text{int}} = 3\gamma_{\text{int}} V_m / d,$$

where V_m is the molar volume and d is the crystallite size. In the nanocrystalline state, β may become stable if $G_\alpha + G_\alpha^{\text{int}} > G_\beta + G_\beta^{\text{int}}$ (Grayznov & Trusov 1993; Datta *et al* 2000a). In other words, if the rate of increase of total free energy ($G + G^{\text{int}}$) with decrease in crystallite size of α phase is higher than that of β phase, the latter will become stable over the former below a critical crystallite size. Figure 16 represents the variation of total free energy, calculated by considering the contribution of interfacial energy, of *fcc* and *hcp* Co nanoparticles with

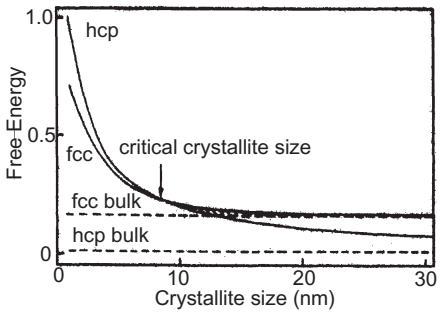

Figure 16. Free energy diagram of *fcc* and *hcp* Co showing the stability of the mentioned phases below and above a critical crystallite size (Ram 2001).

refinement of crystallite size which shows the stability *fcc* Co realtive to *hcp* Co below a critical crystallite size (Ram 2001).

The above condition implies that grains below a critical crystallite size always favour lower interfacial energy, which can be achieved either by formation of an amorphous grain boundary [the crystal/amorphous interfacial energy is small in comparison with intercrystalline interfaces (Desra 1996)] and/or formation of coherent/semicoherent boundaries (Lu 1996; Bianco *et al* 1998; Datta *et al* 2000). Using a Landau–Ginsburg free energy for the evolution of nanograin boundary energy and introducing a topological order parameter of mechanically alloyed intermetallics, Desra (1996, 1997) has proposed the formation of glassy layers below a critical crystallite size. Figure 17 shows a proposed phase diagram of crystallite size vs long-range order parameter for mechanically alloyed Zr_3Al, which exhibits three domains: two domains where nanocrystalline and amorphous phase are stable and a region where the two phases coexist. Bianco *et al* (1998) have explained the formation of close-packed *fcc* structure at the relaxed amorphous grain boundary of nanocrystalline Fe by the possible presence of coherency of the two most-densely packed planes of the two structures. Datta *et al* (2000b) have explained the formation of congruent melting compounds instead of equilibrium non-congruent melting compound in the nanocrystalline state of the Ni–Si system by considering the presence of interfacial energy. It has been proposed that congruent melting compounds formed by polymorphous and eutectic nanocrystallization reactions, controlled by energetic process, exhibit specific orientation relationships between neighbouring nanograins of low energetic configuration

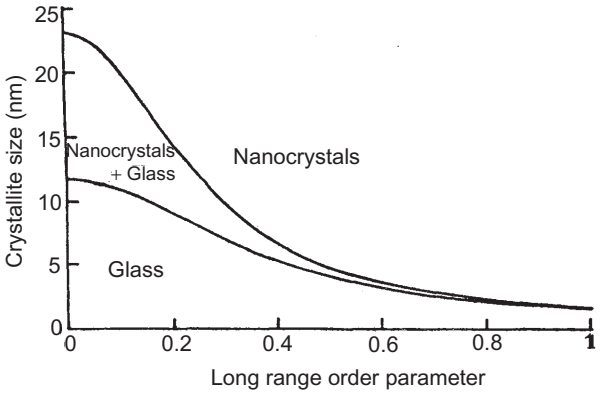

Figure 17. A non-equilibrium phase diagram of Zr_3Al showing the extent of two domains of metastability for the glass and the nanocrystals and a region where the two phases coexist (Desra 1997).

characterized by coherent or semicoherent boundaries (Lu 1996; Datta *et al* 2000). On the other hand, the non-congruent melting compound results of peritectic or peritectoid reactions products, controlled by an atomic diffusion process, always contain randomly oriented nanocrystallites of relatively higher energetic configuration. Thus, the nanocrystalline state appears to favour the congruent melting compounds over the noncongruent melting phases in Ni–Si system below certain crystallite size due to low energy interfaces of the former.

5. Thermal stability of nanocrystalline materials

According to the well-known Gibbs-Thompson equation, the driving force for grain growth process in conventional polycrystals can be expressed as $\Delta\mu = 2\gamma V_a/d$, where V_a is the atomic volume, γ is the interfacial energy, and d is the crystallite size (Sewmon 1997). Due to presence of high density of interfaces and nanometre-sized grains in nanocrystalline materials, it is expected that the grain growth will be extremely large for nanocrystalline materials even at room temperature. However, contrary to the expectations, experimental observations indicate that most nanocrystalline materials of either metals or compounds, synthesized by various methods, exhibit inherent grain size stabilities up to reasonably high temperatures (Suryanarayana 1995; Lu 1996; Malow & Koch 1997; Gleiter 2000; Joardar *et al* 2002). Grain sizes may remain rather stable up to elevated temperatures, sometimes as high as about $\sim$0·4–0·5 T_m, which is comparable with that of grain growth in conventional coarse-grained polycrystals (Suryanarayana 1995; Lu 1996; Malow & Koch 1997; Joardar *et al* 2002). Therefore, inherent grain size stability in nanocrystalline materials presents a challenge to the classical theory for grain growth, that is, whether grain growth in nanocrystalline materials involves the same mechanism as that in coarse-grained polycrystalline materials or involves different "new physics".

Grain growth in conventional polycrystalline materials is considered to be controlled by atomic diffusion in the grain boundary, and its kinetics is frequently described by two significant parameters, namely, Q (activation energy) and m (grain growth exponent) that determine the microscopic mechanism of grain growth (Lu 1996; Gleiter 2000). A number of theoretical treatments suggest that normal grain growth, for high purity metals at high homologous temperature, should ideally occur in a parabolic manner ($m \sim 2$) (Beck *et al* 1948; Malow & Koch 1997; Gleiter 2000) and as grain growth involves the transport of atom across and presumably also along the boundaries, the activation energy (Q) of the process is frequently compared with that of grain boundary diffusion. Investigations on the grain size stability characterized by relatively high grain growth exponent m have been reported in various nanocrystalline materials, including pure metals, oxides, compounds, and composites (Lu 1996; Malow & Koch 1997; Zhou & Guo 1999). Based on measurements on nanocrystalline Cu made by the sliding wear technique, Ganapathi *et al* (1991) indicated that it is difficult to identify grain growth mechanisms on the basis of the exponent m alone, as they can get excellent fits for all values of $m = 2$, 3 or 4. Hofler & Averback (1991) noticed a similar evaluation of the exponent for porous nanocrystalline TiO_2. Activation energies for grain growths in some consolidated nanocrystalline oxides and pure metals (Kumpman *et al* 1993; Wang *et al* 1997) is found to be close to that observed usually for normal grain boundary diffusion in polycrystalline materials. However, in some investigations (Lu 1996; Malow & Koch 1997; Zhou & Guo 1999; Krill *et al* 2001), the activation energy for grain growth in the nanocrystalline materials is consistent with the activation energy for volume diffusion. Lu *et al* (1995) have

observed that the activation energy for grain growth, in a nanocrystalline single-phase $HfNi_5$ sample prepared by melt quenching, is very close to the value for volume diffusion of Hf. The agreement between the activation energy for nanocrystalline grain growth and that for volume self-diffusion (Lu 1996; Krill *et al* 2001; Lu *et al* 1995) implies that there might be a volume diffusion process during growth of the nanometre-sized crystallites in addition to interface diffusion.

The above discussion implies that the growth process of nanometre-sized grains is not controlled solely by the Zener drag mechanism. Other mechanisms such as pinning of grain boundaries by pores, inclusions, triple junctions or segregation of lower density solute at grain boundary may also be operative (Suryanarayana 1995; Lu 1996; Malow & Koch 1997; Michels *et al* 1999; Gleiter 2000). The fact that pores and impurity doping have considerable effect on the grain growth characteristics was demonstrated in TiO_2. For an initial grain size of 14 nm, when the porosity was about 25%, the grain size (after annealing for 20 h at 973 K) was 30 nm (Hahn *et al* 1990). When the porosity was reduced to about 10%, grain size with similar annealing treatment was dramatically increased to 500 nm. Similarly, pinning of grain boundaries in nanocrystals of a Ni solid solution by the Ni_3P precipitates in a crystallized Ni–P amorphous alloy (Boylan *et al* 1991; Lu 1996), segregation of Si to grain boundaries in a Ni–Si solid solution (Knauth *et al* 1993) and segregation of Zr to grain boundaries in Pd–Zr solid solution (Krill *et al* 1995) have been identified as being responsible for preventing grain growth in nanocrystalline phases. Therefore, grain size stability in nanocrystalline materials has been found to be closely related to the structural characteristics of the material, such as grain size and its distribution, grain morphologies, triple junctions, porosity in the sample, and so on.

Recent reports suggest that the lowering of interfacial energy with grain refinement (Lu *et al* 1993; Weismuller 1994; Krill *et al* 1995; Lu 1996; Datta *et al* 2000; Gleiter 2000) and lattice strain in nanometre-sized crystallites (Lu 1996; Kumpmann *et al* 1993; Lu *et al* 2000; Datta *et al* 2001) may also play an important role in controlling grain size stability of nanocrystalline materials. For example, Lu *et al* (1993) studied the thermal stability of 7–48 nm grains in Ni–P alloy and interestingly noticed that samples with smaller grain sizes have enhanced thermal stabilities, suggesting that grain growth temperature and activation energy for growth in a nanocrystalline state are higher in comparison with that in coarser grains. Similarly, in nanocrystalline materials consisting of nanometre-sized crystallites (TiN) embedded in an amorphous matrix (amorphous Si_3N_4), rate of crystal growth was observed to decrease with crystal size (Veprek *et al* 1999). In a number of systems, significant grain growth has been noticed at the onset of metastable to stable phase transformation (Ding & Liu 1997; Datta *et al* 2000c; Gleiter 2000). In Ni–Si alloys, prepared by high energy ball-milling, the onset of grain growth and the nucleation of the stable phase has been observed (Datta *et al* 2000c). Figure 18 shows the grain coarsening and strain relaxation behaviour of metastable phase mixtures of Ni(Si) and γ-$Ni_{31}Si_{12}$ phases (Ni-25at.%Si) with increase in temperature. The increase of crystallite size with temperature is very small for both Ni(Si) and γ-$Ni_{31}Si_{12}$ (from 10 and 17 nm in the as milled state to 40 and 50 nm at 673 K for Ni(Si) and γ-$Ni_{31}Si_{12}$, respectively). Once the crystallite size of γ-$Ni_{31}Si_{12}$ and Ni(Si) reaches about 50 nm, they react with each other to form equilibrium non-congruent ordered Ni_3Si. The results indicate that crystallite size of ordered Ni_3Si is about 135 nm at the temperature of formation (723 K), which suggests that the grain growth is very fast for this phase and it is probably stable only in the bulk state (above 100 nm). Similarly, significant grain growth has been reported at the onset of metastable anatase to rutile phase transformation (Ding & Liu 1997). In a recent study, Joardar *et al* (2002) has identified that the onset of grain growth of

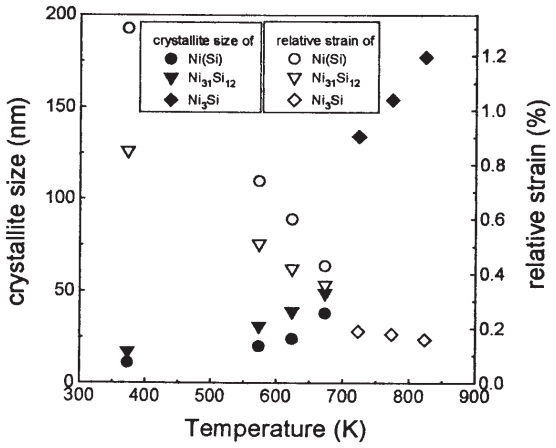

Figure 18. Average crystallite size and lattice strain of Ni(Si), $Ni_{31}Si_{12}$ and ordered Ni_3Si as a function of annealing temperature of mechanically alloyed Ni-25 at. %Si composition (Datta *et al* 2000c).

disordered NiAl(Fe)/NiAl(Cr) occurs when the ordering parameter reaches a saturated value $\sim$ 0·7, that is after transformation to a more or less equilibrium state (see figure 19). This abnormal phenomenon of grain size dependence of stability in the nanocrystalline samples seems to originate from the configuration and the lower energetic state of the interfaces in the nanocrystalline state.

Similarly, the lattice strain of nanometre-sized crystallites has been identified as having direct effect on their stability. Most of the experimental results (Lu 1996; Bonetti 1999; Lu *et al* 2000; Datta *et al* 2001) showed that the strain release process in nanocrystalline samples always occurs prior to or simultaneously with grain growth process, which suggests that the lattice distortion of nanometre-sized crystallite also plays an important role in controlling the grain-size stability of nanocrystalline materials. Figure 20 shows the variation of crystallite size and the molar volume of distorted *fcc* Ni(Si) of molar volume 6·93 cm^3/mol

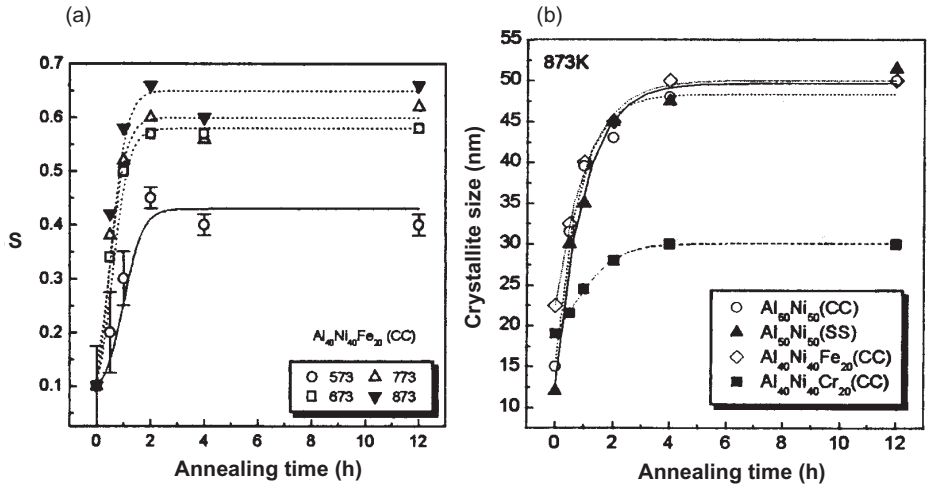

Figure 19. Variation of **(a)** long range order parameter, *S* and **(b)** crystallite size during thermal treatment of as milled Al-40 at. %Ni-20 at. %Fe (Joardar *et al* 2002).

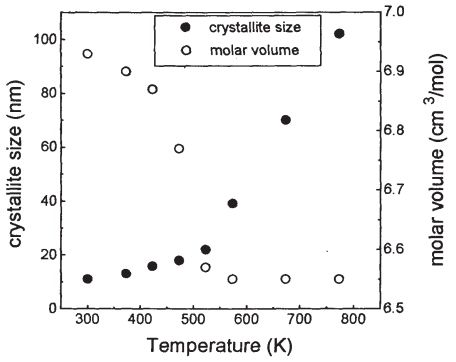

Figure 20. Variation of crystallite size and molar volume of *fcc* Ni(Si) with annealing temperature (Datta *et al* 2001).

with increase in temperature. The crystallite size increases very slowly up to 523 K (22 nm at 523 K, as compared 11 nm in the as-milled state), while the molar volume drops from 6·93 to 6·57 cm^3/mol, which is close to the equilibrium molar volume of 5at.% solid solution of Si in Ni (6·55 cm^3/mol). Above this temperature, substantial grain growth is observed (from 22 nm at 523 K to 39, 70 and 100 nm at 573, 673 and 773 K respectively), while the molar volume decreases only marginally to 6·55 cm^3/mol after heating to 573 K and remains constant on further heating up to 773 K. The change of distorted lattice to equilibrium configuration is expected to arise through atomic diffusion, not only along the interfaces but also necessarily inside the crystallite lattice. Thus, grain growth in nanocrystalline materials is expected to be the result of both interface and volume diffusion. Recent theoretical considerations (Czubayko *et al* 1998; Estrin *et al* 1999, 2000) present a compelling case for enhanced intrinsic stability with respect to coarsening in materials with nanometre-sized grains. These theoretical models indicate the existence of a critical grain size (d_c), below which the rate controlling step for grain-boundary migration is not the boundary curvature driven diffusion of atoms across and along the boundary, but the migration and/or rearrangement of other features associated with the grain boundaries, like triple junctions or excess volume localized in the core regions (Czubayko *et al* 1998; Estrin *et al* 1999). Estrin *et al* (1999, 2000) point out that, at sufficiently small grain sizes, the rate-controlling step for boundary migration is transport of excess volume, located at the grain boundary, away from the moving boundaries. Since grain growth entails a reduction in the total grain-boundary area, the excess volume localized in the annihilated boundary area must be accommodated elsewhere in the sample or transported to the surface. According to recent computer simulations performed by Upmanyu *et al* (1998), much of the excess volume freed during grain growth is initially incorporated into nearby crystalline regions in the form of vacancies, leading to a nonequilibrium vacancy concentration and a concomitant increase in the free energy, G, which counteracts the decrease in G associated with the reduction in area. A feature of such models is the prediction of a linear dependence of d on annealing time t when $d < d_c$ and a crossover at $d = d_c$ to the nonlinear growth kinetics familiar from studies of grain growth in conventional materials. Thus, when grain growth is controlled by the redistribution of excess volume (below d_c), the activation energy should be much higher (close to self-diffusion) than that of grain growth in a coarse-grained specimen of the same material (grain boundary diffusion). The feature of this model, that is the linear growth kinetics below a critical crystallite size, is in good agreement with recent experimental work performed by Krill *et al* (2001) on nanocrystalline Fe.

References*

Ayyub P, Multani M S, Barma M, Palkar V R, Vijayaraghavan R 1988 *J. Phys.* C21: 2229
Ayyub P, Palkar V R, Chattopadhyay S, Multani M 1995 *Phys. Rev.* B51: 6135
Balogh J, Bujdoso L, Kaptas D, Kemeny T, Vincze I, Szabo S, Beke D L 2000 *Phys. Rev.* B61: 4109
Beck Ch, Haertl W, Hempelmann R 1999 *J. Mater. Res.* 13: 3174
Beck P A, Kramer J C, Demer L J, Holzworth M L 1948 *Trans. AIME* 175: 372
Bonetti E, Bianco L Del, Pasquini L, Sampaolesi E 1999 *Nanostruct. Mater.* 12: 685
Boylan K, Ostrander D, Erb U, Palumbo G, Aust K T 1991 *Scr. Metall. Mater.* 25: 2711
Chanderis D, Magnan H, Jezequel G, Hricovinim K, Rossi G, Villette B, Lacante J 1990 *Phys. Scr.* T31: 239
Chatterjee P P, Pabi S K, Manna I 1999 *J. Appl. Phys.* 86: 5912
Chattopadhay P P, Nambissan P M G, Pabi S K, Manna I 2001 *Phys. Rev.* B63: 054107
Chraska T, King A H, Berndt C C 2000 *Mater. Sci. Eng.* A286: 169
Czubayko U, Sursaeva V G, Gottstein G, Shvindlerman L S 1998 *Acta. Mater.* 46: 5863
Datta M K 2001 *Synthesis and characterization of nanocrystalline silicides by mechanical alloying in Fe–Ni–Si system*. Ph D thesis, Indian Institute of Technology, Kharagpur
Datta M K, Pabi S K, Murty B S, 2000a *J. Mater. Res.* 15, 1429
Datta M K, Pabi S K, Murty B S 2000b *J. Appl. Phys.* 87: 8393
Datta M K, Pabi S K, Murty B S 2000c *Mater. Sci. Eng.* A284: 219
Datta M K, Pabi S K, Murty B S 2002 *J. Mater. Res.* (communicated)
Datta M K, Pabi S K, Murty B S 2001 *Philos. Mag. Lett.* 81: 77
del Bianco L, Hernando A, Bonetti E, Navarro E 1997 *Phys. Rev.* B56: 8894
del Bianco L, Ballesteros C, Rojo J M, Hernando A, 1998 *Phys. Rev. Lett.* 81: 4500
Desra P J 1996 *Philos. Mag.* A74: 103
Desra P J 1997 *Nanostruct. Mater.* 8: 687
Ding X Z, Liu X H 1997 *J. Alloys Compounds* 248: 143
Eastman J A, Fitzsimmons M R 1995 *J. Appl. Phys.* 77: 522
Estrin Y, Gottstein G, Shivindlerman L S 1999 *Scr. Mater.* 41: 385
Estrin Y, Gottstein G, Rabkin E, Shivindlerman L S 2000 *Scr. Mater.* 43: 141
Ettl C, Samwer K 1994 *Mater. Sci. Eng.* A178: 245
Fecht H J 1992 *Nature (London)* 356: 133
Frase H N, Fultz B, Roberts J L, Spooner S 2000 *Philos. Mag.* B80: 1545
Fukunaga T 1995 *Physica* B213&214: 518
Gaffet E, Faudot F, Harmelin M 1991 *Mater. Sci. Eng.* A149: 85
Gaffet E, Malhouroux N, Abdellaoui M 1993 *J. Alloys Compounds* 194: 339
Gaffet E, Hermalin H 1990 *J. Less Common Met.* 157: 201
Gamarnik M Ya 1991 *Phys. Status Solidi* B168: 389
Ganapathi S K, Owen D M, Chokshi A H 1991 *Scr. Metall. Mater.* 25: 2699
Garvie R C 1965 *J. Phys. Chem.* 69: 1298
Gleiter H 1995 *Nanostruct. Mater.* 6: 3
Gleiter H 1981 *Deformation of polycrystals: Mechanisms and microstructures* (eds) N Hansen, A Horsewell, T Leffers, H Lilhot (Denmark: Riso National Laboratory) p. 15
Gleiter H 2000 *Acta Mater.* 48: 1
Grayznov V G, Trusov L I 1993 *Prog. Mater. Sci.* 37: 289
Guo F Q, Lu K 1998 *Philos. Mag. Lett.* 77: 181
Hadjipanayis G C, Siegel R W 1994 *Nanophase materials: Synthesis-properties-applications* (Dordrecht: Kluwer Academic)
Hague D C, Mayo M J 1997 *J. Am. Ceram. Soc.* 80: 149

*References in this list are not in journal format

Hahn H, Logas J, Averback R S 1990 *J. Mater. Res.* 5: 609
Hahn H, Logas J, Averback R S 1990 *J. Mater. Res.* 5: 609
Haubold T, Birringer R, Lengeler B, Gleiter H 1989 *Phys. Lett.* A135: 461
Herr U, Geigl M, Samwer K 1998 *Philos. Mag.* A77: 641
Herr U, Jing J, Gonser U, Gleiter H 1990 *Solid State Commun.* 76: 192
Hodaj F, Desra P J 1996 *Acta Mater.* 44: 4485
Hofler H J, Averback R S 1991 *Scr. Metall. Mater.* 24: 2401
Hong L B, Ahn C C, Fultz B 1995 *J. Mater. Res.* 10: 2048
Ikeda H, Qi Y, Cagin T, Samwer K, Johnson W L, Goddward W A 1999 *Phys. Rev. Lett.* 82: 2900
Joardar J, Pabi S K, Fecht H J, Murty B S 2002 *Philos. Mag. Lett.* (accepted)
Johnson W L, Li M, Krill C E III 1993 *J. Non-Cryst. Solids* 156-158: 481
Johnson W L, Fecht H J 1988 *J. Less Common Met.* 145: 63
Kanters J, Eisele U, Rodel J 2000 *Acta Mater.* 48: 1239
Keblinski P, Wolf D, Phillpot S R, Gleiter H 1999 *Scr. Mater.* 41: 631
Kim H S, Estrin Y, Bush M B 2000 *Acta Mater.* 48: 493
Klassen T, Herr U, Averback R S 1997 *Acta Mater.* 45: 2921
Knauth P, Charai A, Gas P 1993 *Scr. Metall. Mater.* 28: 325
Koch C C 1996 *Scr. Mater.* 34: 21
Koch C C 1997 *Nanostruct. Mater.* 9: 13
Koike J 1993 *Phys. Rev.* B47: 7700
Krill C E, Helfen L, Michels D, Natter H, Fitsch A, Masson O, Birringer R 2001 *Phys. Rev. Lett.* 86: 842
Krill C E, Klen R, Janes S, Birringer R 1995 *Mater. Sci. Forum.* 179-181: 443
Kumpmann A, Gunther B, Kunze H D 1993 *Mater. Sci. Eng.* A168: 165
Lai S L, Guo J Y, Petrova V, Ramanath G, Allen L H 1996 *Phys. Rev. Lett.* 77: 99
Liao S C, Chen Y J, Kear B H, Mayo W E 1998 *Nanostruct. Mater.* 10: 1063
Liao S C, Chen Y J, Mayo W E, Kear B H 1999 *Nanostruct. Mater.* 11: 553
Liu C L, Adams J B, Siegel R W 1994 *Nanostruct. Mater.* 4: 265
Liu X D, Lu K, Zhang H Y, Hu Z Q 1994 *J. Phys. Condens. Mater.* 6: L497
Loffler J, Weissmuller J, Gleiter H 1994 *Nanostruct. Mater.* 6: 567
Loffler J, Weissmuller J 1995 *Phys. Rev.* B52: 7076
Lu K 1996 *Mater. Sci. Eng.* R16: 161
Lu K, Luck R, Predel B 1993 *Scr. Metall. Mater.* 28: 1387
Lu K, Sun N X 1997 *Philos. Mag. Lett.* 75: 389
Lu K, Zhao Y H 1999 *Nanostruct. Mater.* 12: 559
Lu K, Dong Z F, Bakony I, Cziraki A 1995 *Acta Metall. Mater.* 43: 2641
Lu K, Luck R, Predel B 1993 *Scr. Metall. Mater.* 28: 1387
Lu L, Wang L B, Ding B Z, Lu K 2000 *Mater. Sci. Eng.* A286: 125
Malow T R, Koch C C 1997 *Acta Mater.* 45: 2177
Michels A, Krill C E, Ehrhardt H, Birringer R, Wu D T 1999 *Acta Mater.* 47: 2143
Murty B S, Ranganathan S 1998 *Int. Mater. Rev.* 43: 101
Mutschele T, Kirchheim R 1987 *Scr. Metall.* 21: 1101
Pabi S K, Das A 1997 *Met. Mater. Process.* 9: 229
Pabi S K, Joardar J, Murty B S 2001 *Proc. Indian. Natl. Sci. Acad.* A67: 1
Phillpot S R, D Wolf, H Gleiter 1995 *J. Appl. Phys.* 78: 847
Qin W, Chen Z H, Huang P Y, Zhuang Y H 1999 *J. Alloys Compounds* 292: 230
Ram S 2001 *Acta Mater.* 49: 2297
Roco M C, Williams R S, Alivisatos P (eds) 2000 *Nanotechnology research directions: IWGN workshop report–vision for nanotechnology in the next decade* (Dordrecht: Kluwer Academic)
Roco M C, Bainbridge W S 2001 *Societal implications of nanoscience and nanotechnology* (Dordrecht: Kluwer Academic)
Schmidt M, Kusche R, Issendorff B V, Haberland H 1998 *Nature (London)* 393: 238

Seigel R W, Hu E, Roco M C (eds) 1999 *Nanostructure science and technology: R & D Status and Trends in Nanoparticles, Nanostructured materials and Nanodevices* (Dordrecht: Kluwer Academic)
Sewmon P G 1969 *Transformation in metals* (New York: McGraw-Hill) p. 300
Stern E A, Siegel R W, Newville M, Sanders P G, Haskel D 1995 *Phys. Rev. Lett.* 75: 3874
Suryanarayana C 2001 *Prog. Mater. Sci.* 46: 1
Suryanarayana C 1995 *Int. Mater. Rev.* 40: 41
Swygenhoven H V, Farkas D, Caro A 2000 *Phys. Rev.* B62: 831
Terwilligner C D, Chiang Y M 1993 *MRS Symp. Proc.* 289: 15
Upmanyu M, Srolovitz D J, Shvindlerman L S, Gottstein G 1998 *Interface Sci.* 6: 287
Veprek S, Iqbal Z, Sarott F A 1982 *Philos. Mag.* B45: 137
Veprek S, Nesladek P, Niederhofer A, Mannling H, Jilnek M 1999 *TMS Annual Meeting*, San Diego, CA
Wang N, Wang Z, Aust K T, Erb U 1995 *Acta Metall. Mater.* 43: 519
Wang N, Wang Z, Aust K T, Erb U 1997 *Acta Mater.* 45: 1655
Weissmuller J, Krauss W, Haubold T, Birringer R, Gleiter H 1992 *Nanostruct Mater.* 1: 439
Weissmuller J 1994 *J. Mater. Res.* 9: 4
Wolf D, Wang J, Phillpot S R, Gleiter H 1995 *Phys. Lett.* A205: 274
Yamada K, Koch C C 1993 *J. Mater. Res.* 8: 1317
Yavari A R, Desra P J, Benameur T 1992 *Phys. Rev. Lett.* 68: 2235
Yavari A R 1994 *Mater. Sci. Eng.* A179/180: 20
Zhao Y H, Lu K, Liu T 1999 *Phys. Rev.* B59: 11117
Zhao Y H, Lu K 1997 *Phys. Rev.* B56: 14330
Zhou L Z, Guo J T 1999 *Scr. Mater.* 40: 139
Zhu B H, Averback R S 1996 *Philos. Mag. Lett.* 73: 27
Zhu X, Birringer R, Herr U, Gleiter H 1987 *Phys. Rev.* B30: 9085